Bioorganic & Medicinal Chemistry 16 (2008) 7450–7456

Contents lists available at ScienceDirect

Bioorganic & Medicinal Chemistry

journal homepage: www.elsevier.com/locate/bmc

Homo- and hetero-bivalent edrophonium-like ammonium salts as highly potent, dual binding site AChE inhibitors

Francesco Leonetti, Marco Catto, Orazio Nicolotti, Leonardo Pisani, Anna Cappa, Angela Stefanachi, Angelo Carotti *

Dipartimento Farmaco-Chimico, Università di Bari, via Orabona 4, I-70125 Bari, Italy

ARTICLE INFO

Article history:
Received 28 February 2008
Revised 3 June 2008
Accepted 6 June 2008
Available online 14 June 2008

Keywords:
Edrophonium-like ammonium salts
Selective acetylcholinesterase inhibitors
Butyrylcholinesterase inhibition
Molecular docking

ABSTRACT

A number of mono- and bis-quaternary ammonium salts, containing edrophonium-like and coumarin moieties tethered by an appropriate linker, proved to be highly potent and selective dual binding site acetylcholinesterase inhibitors with good selectivity over butyrylcholinesterase. Homobivalent bis-quaternary inhibitors **11** and **12**, differing by only one methylene unit in the linker, were the most potent and selective inhibitors exhibiting a sub-nanomolar affinity (IC_{50} = 0.49 and 0.17 nM, respectively) and a high butyryl-/acetylcholinesterase affinity ratio (SI = 1465 and 4165, respectively). The corresponding hetero-bivalent coumarinic inhibitors **13** and **14** were also endowed with excellent inhibitory potency but a lower AChE selectivity (IC_{50} = 2.1 and 1.0 nM, and SI = 505 and 708, respectively). Docking simulations enabled clear interpretation of the structure–affinity relationships and detection of key binding interactions at the primary and peripheral AChE binding sites.

1. Introduction

In vertebrates two enzymes, acetylcholinesterase (AChE) and butyrylcholinesterase (BChE), efficiently catalyze acetylcholine hydrolysis. They are distinguished on the basis of substrate specificity, tissue distribution, and sensitivity to inhibitors.[1] AChE is predominant in the muscle and nervous system, and plays a fundamental role in impulse transmission by terminating the action of the neurotransmitter acetylcholine at the cholinergic synapses and neuromuscular junctions.[2]

AChE inhibitors have found widespread use in the treatment of different pathologies, such as Alzheimer's disease (AD), glaucoma, neuromuscular blockade in surgical anesthesia, and myasthenia gravis.[3] Although the degree of similarity between AChE and BChE is high (51–54% of identity and 70–72% homology), their physiological and pathological roles only partly overlap. Therefore, the discovery of selective AChE or BChE inhibitors, and of dual inhibitors as well, is intensely pursued.[4] Nowadays, these studies are extremely facilitated by the availability of high-resolution X-ray crystal structures of many AChE–inhibitor complexes. The three-dimensional structure of AChE has been first determined on *Torpedo californica* (*Tc*),[5] and since then many other complexes with structurally diverse inhibitors and AChE from different species have been determined and reported in the Protein Brookhaven Database (PDB).[6] The most interesting structural aspects of these isoenzymes are the presence of a deep narrow gorge, at the bottom of which the catalytic triad is found, and of a regulatory site, called the peripheral anionic site (PAS), at the entrance of the gorge. PAS is absent in BChE, which might explain, at least in part, some observed substrate/inhibitor specificities. Most of the reported AChE inhibitors interact with the primary or peripheral binding site, or both. Compounds such as edrophonium and tacrine (Chart 1) act exclusively at the primary binding site, whereas others such as propidium and fasciculin act at the PAS, and bis-quaternary ammonium salts (e.g., decamethonium) as well as diverse homo- and hetero-bivalent mono- and bis-protonated amines act at both.[7,8]

Recently, different groups have successfully improved the enzyme affinity of monovalent AChE inhibitors, such as tacrine and (−)-huperzine A, by synthesizing homo- and hetero-bivalent derivatives with binding moieties placed at the appropriate distance to efficiently interact with both binding sites.[9–11] It is worth noting that binding at the PAS can be triggered also by non-ionic interactions, that is, π–π stacking and hydrophobic interactions, as in the case of donepezil,[12] an efficient AChE inhibitor currently used in the treatment of AD.[13]

Some years ago, some of us published the synthesis and biological evaluation of a series of 7-substituted coumarins displaying dual AChE-monoamineoxidase (MAO) inhibitory activity.[14] The absence of basic (protonable) or quaternary nitrogen atoms in these compounds, the prevalent hydrophobic character of the

* Corresponding author. Tel.: +39 080 544 2782; fax: +39 080 544 2230.
E-mail address: carotti@farmchim.uniba.it (A. Carotti).

0968-0896/$ - see front matter © 2008 Elsevier Ltd. All rights reserved.
doi:10.1016/j.bmc.2008.06.022

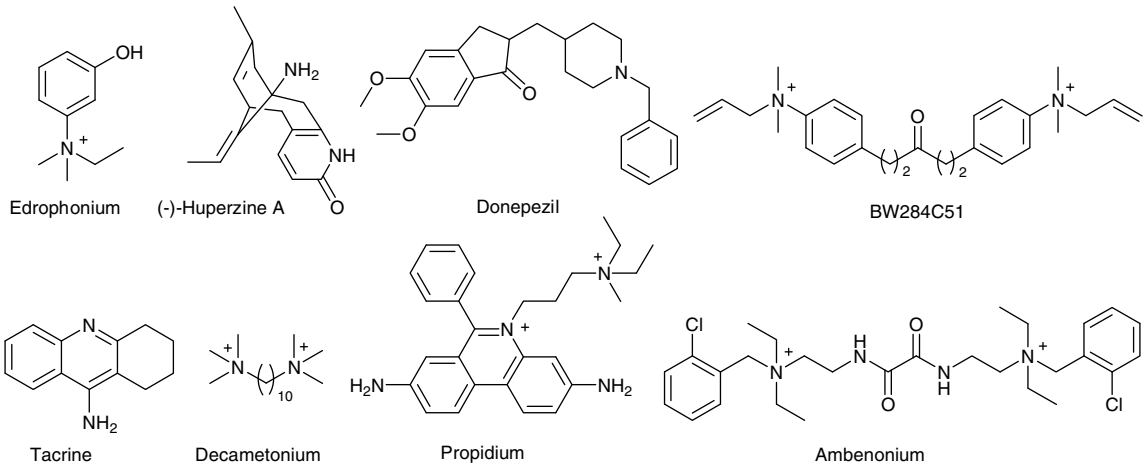

Chart 1. Chemical structures of some cited AChE inhibitors.

substituted coumarin ring, and preliminary molecular docking simulations suggested that their AChE inhibitory activity might arise from an interaction at the PAS. To recover additional and efficient binding at the primary binding site potentially capable of enhancing the low AChE inhibitory potency of our coumarin derivatives, we designed and prepared a small library of potential dual binding site AChE inhibitors, depicted in Chart 2, through a solid-phase approach.

We reasoned that an additional and efficient interaction with the primary binding site might be triggered by the introduction of an edrophonium-like moiety (a trimethyl- instead of the dimethylethyl-ammonium group of edrophonium was used) at a suitable distance from the coumarin nucleus. Indeed, tethering two low-affinity ligands with a linker of appropriate chemical nature and length has resulted in a successful strategy to strongly improve protein binding affinity and lays the groundwork for a 'fragment-based' design strategy.[15] Moreover, we designed and tested also homobivalent bis-quaternary ammonium salts containing edrophonium-like cationic moiety.

2. Chemistry

Within the strategic framework delineated above, we designed and prepared compounds **1**–**15** (Table 1) through solid-phase synthesis on a Wang resin, starting from a mono-TiPS-protected 3,5-dihydroxy-*N*-methyl (or -benzyl) aniline, as reported in Scheme 1 and already previously described by our group.[16] Compound **16**, a dideoxy-analogue of **14** was prepared according to a traditional solution phase synthesis as reported in Scheme 2. Since data from literature suggested that an appropriate distance between the two potentially binding moieties (i.e., coumarin and edrophonium-like

Table 1
AChE and BChE inhibition data of compounds **1**–**16** and reference leads 3-HBT and DMC[a]

Compound	R	R^1	*n*	Y	AChE[b]	BChE[b]	SI
1	CH_3	CH_3	3	OH	1905	nd	—
2	CH_3	CH_3	4	OH	6456	25%	—
3	Bn	CH_3	3	OH	6166	nd	—
4	Bn	CH_3	4	OH	40%	nd	—
5	Bn	Bn	3	OH	3%	nd	—
6	Bn	Bn	4	OH	14%	nd	—
7	CH_3	—	3	OH	871	nd	—
8	CH_3	—	4	OH	275	25%	—
9	Bn	—	3	OH	8%	nd	—
10	Bn	—	4	OH	15%	nd	—
11	CH_3	CH_3	3	OH	0.49	718	1465
12	CH_3	CH_3	4	OH	0.17	715	4165
13	CH_3	—	3	OH	2.1	1060	505
14	CH_3	—	4	OH	1.0	708	708
15	Bn	CH_3	4	OH	6560	42%	—
16	CH_3	CH_3	4	H	158	2344	15
	3-HBT				12,000	13%	—
	DMC				42,000	25%	—

[a] R, R^1, *n*, and Y refer to the chemical structures shown in Chart 2; SI is the selectivity index (see text).
[b] Inhibition data (relative SEM <10%) are expressed as IC_{50} (nM) or as percentage of inhibition at 10 μM for AChE (except for compound **5**, 50 μM) and 50 μM for BChE (except for compounds **15**, 3-HBT and DMC, 10 μM); nd, not determined.

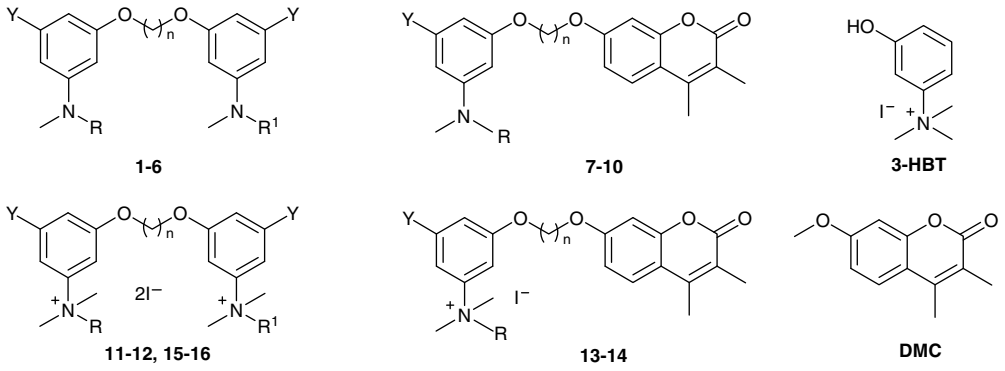

Chart 2. Chemical structures of targeted homo- and hetero-bivalent AChE inhibitors **1**–**16** and reference leads 3-HBT and DMC. (Y = H, OH; R and R^1 = CH_3 and $C_6H_5CH_2$; *n* = 3, 4: see Table 1).

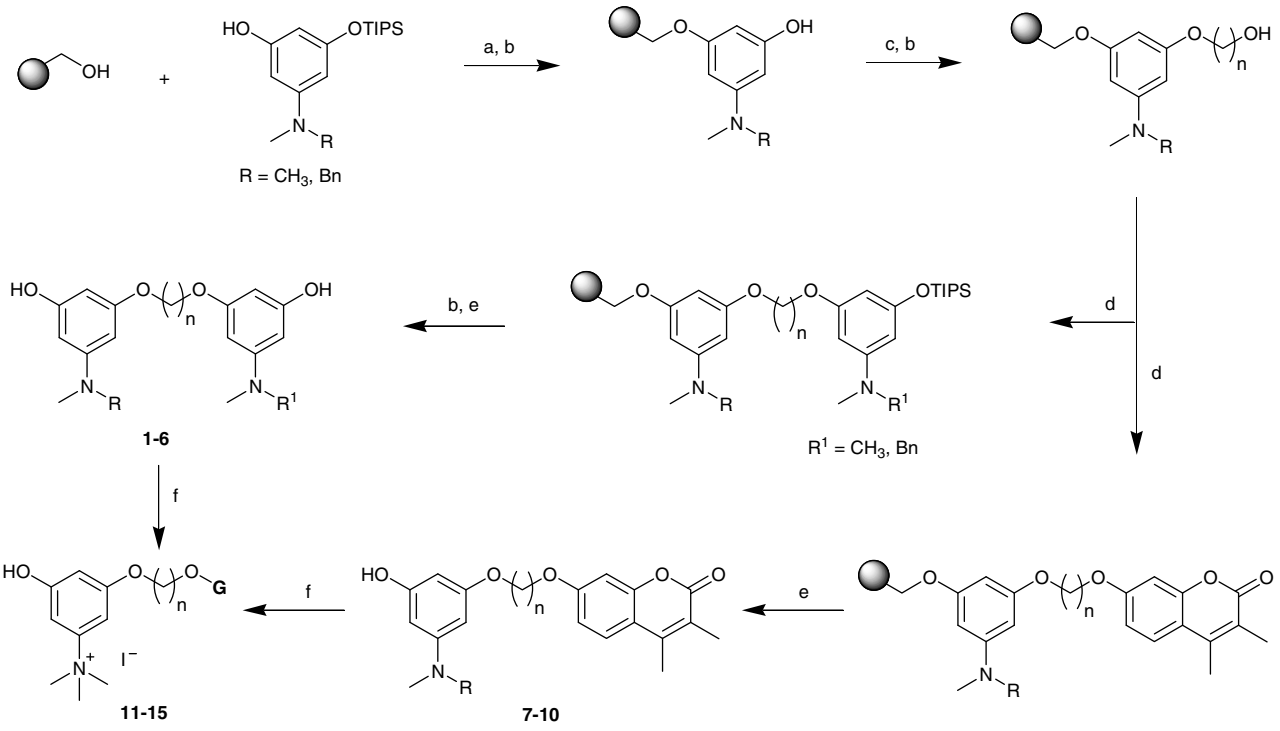

Scheme 1. Solid-phase synthesis of compounds **1**–**15**. Reagents and conditions: (a) PPh_3, DIAD, THF; (b) TBAF, THF; (c) PBu_3, ADDP, CH_2Cl_2, 3-{[*tert*-butyl(dimethyl)silyl]oxy}propan-1-ol or 4-{[*tert*-butyl(dimethyl)silyl]oxy}butan-1-ol; (d) PBu_3, ADDP, CH_2Cl_2, 3-(dimethylamino)-5-[(triisopropylsilyl)oxy]phenol or 3,4-dimethyl-7-hydroxycoumarin; (e) TFA, CH_2Cl_2; (f) CH_3I, CH_3CN, **1**, **2** and **4**, or **7** and **8**. **G**: 3-hydroxy-5-(trimethylammonium)phenyl iodide (**11** and **12**), 3-hydroxy-5-(*N*-benzyl-*N*,*N*-dimethylammonium)phenyl iodide (**15**) and 3,4-dimethylcoumarin (**13** and **14**).

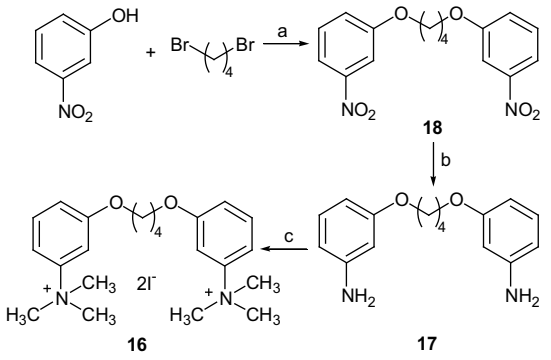

Scheme 2. Synthesis of compound **16**. Reagents and conditions: (a) K_2CO_3, CH_3CN, reflux; (b) H_2, Pd 'black', EtOH/dioxane 1:1, rt; (c) K_2CO_3, CH_3I, EtOH, reflux.

moieties) might be reached by linking the two phenolic hydroxyls with 3 or 4 methylene groups, compounds **1–16** were prepared and tested as cholinesterase inhibitors along with two reference compounds 3-hydroxy-*N*,*N*,*N*-trimethylbenzenaminium iodide (3-HTB) and 3,4-dimethyl-7-methoxycoumarin (DMC) (Chart 2).

3. Biological assays

Compounds **1**–**16** and reference leads 3-HBT and DMC, were tested as cholinesterase inhibitors on bovine acetylcholinesterase and equine serum butyrylcholinesterase according to the specPro-photometric method of Ellman.[17] Inhibition data are reported in Table 1 as IC_{50} mean values resulting from at least three independent measures. Less active compounds were tested at 50 or 10 μM, according to their solubility in the assay medium, and their activity, expressed as percent of inhibition at a given concentration are reported in Table 1 along with the chemical structures of all the compounds examined.

4. Results and discussion

At a glance, the data in Table 1 show that our design led to an outstanding improvement of the AChE inhibitory potencies of the separate 3-HTB and DMC moieties, which presented IC_{50} values equal to 12,000 and 42,000 nM, respectively. Indeed, mono-quaternary (**13** and **14**) and bis-quaternary (**11** and **12**) ammonium salts were endowed with an outstanding AChE affinity (from nanomolar to sub-nanomolar IC_{50}) and an excellent AChE selectivity (from 505 to 4165 SI, where SI is the selectivity index, that is, the IC_{50}BChE/IC_{50} AChE affinity ratio). Noticeably, the most active and selective AChE bis-quaternary homobivalent inhibitors **11** and **12** differ only by one methylene unit in the spacer length and their sub-nanomolar affinities are close (IC_{50} = 0.49 and 0.17 nM, respectively). Interestingly, bis-quaternary homobivalent inhibitor **12** showed an inhibitory potency almost identical to that of Ambenonium, (IC_{50} = 0.17 and 0.12 nM, respectively)[18] and much better than BW284C51 (IC_{50} = 8 nM),[19] two of the most potent bis-quaternary ammonium salts described so far (Chart 1).

Moreover, the hetero-bivalent mono-quaternary ammonium salts **13** and **14** also showed impressive AChE affinity likely arising from strong interactions between both the coumarin and 3-HTB moieties and the PAS and catalytic binding site, respectively. In particular, the AChE inhibitory activity of **14** (IC_{50} = 1.0 nM) was 12,000- and 42,000-fold higher than that of the single separate moieties, 3-HBT and DMC, respectively.

The strategy of designing dual binding site AChE inhibitors by joining two AChE binding molecules, used previously by diverse authors,[9–11] led also to the discovery of very potent inhibitors, but their starting separate moieties (e.g., tacrine and (−)-huperzine A) already displayed an affinity in the high nanomolar range

(IC_{50} = 134 and 74 nM, respectively, on bovine AChE).[20] In our case, the AChE affinity of the two separate lead molecules was very low and the observed increase of affinity in compounds **13** and **14** was dramatic.

Many other interesting insights emerged from the analysis of the inhibitory potencies of compounds **1**–**15**. As expected, the quaternary ammonium salts were always much more active than the parent amines (compare affinities of **1** and **11**; **2** and **12**; **7** and **13**; **8** and **14**, and **4** and **15**). In fact, although the coumarin ring might engage multiple strong interactions with the enzyme (i.e., hydrophobic and/or π–π stacking interactions, and hydrogen bonds), inhibitor **8**, the most active derivative of the aminic series, was 275-fold less potent than its corresponding quaternary ammonium salt **14** (IC_{50} = 275 vs 1.0 nM). The highest AChE inhibitory activity was observed for bis-quaternary homobivalent derivative **12**, which displayed an inhibitory potency in the sub-nanomolar range (IC_{50} = 0.17 nM) and a very high AChE selectivity (SI = 4165). Homobivalent bis-quaternary ammonium salts **11** and **12** were more active than the corresponding mono-quaternary hetero-bivalent congeners **13** and **14**, whereas opposite results were observed when comparing parent aminic derivatives (i.e., **1** and **7**, and **2** and **8**).

The length of the spacer linking the two moieties binding at the catalytic and peripheral binding sites influenced the observed AChE affinity. Among medium- and highly potent inhibitors, those with four-methylene units were always slightly more potent than the corresponding derivatives with three methylene units (**8** > **7**; **12** > **11** and **14** > **13**). This result suggested that an appropriate distance for a more efficient binding at both the catalytic and peripheral binding sites was provided by a linker of that length. The lowest active AChE inhibitors were the bis-*N*-methyl-*N*-benzylamine derivatives **5** and **6**, with the former yielding only 3% AChE inhibition at 50 μM. Mono *N*-methyl-*N*-benzylamine derivatives were also less active than the corresponding *N*,*N*-dimethylamine derivatives, as can be observed from the following comparisons: **3** < **1**, **4** < **2**, **9** < **7**, and **10** < **8**. The low inhibitory potencies of *N*-benzylamine derivatives may be ascribed to possible steric effects at the AChE binding sites.

An additional investigation was undertaken to assess the role played by the phenolic hydroxyl(s) of the 3-HTB moieties in the binding at the primary and peripheral binding sites of AChE. To this end, we prepared compound **16**, which lacked both the phenolic hydroxyls compared to the highly potent inhibitor **12** according to the synthetic pathways shown in Scheme 2. The AChE inhibitory activity of **16** was dramatically lowered (IC_{50} = 158 nM from 0.17 nM of **12**), while the BChE inhibitory activity was decreased to a much lower extent (IC_{50} = 2344 nM from 715 nM). These findings suggested that the phenolic hydroxyl group of the 3-HTB moieties plays indeed a key role in ligand binding at the catalytic site of AChE, as already observed in the X-ray crystallographic structure of edrophonium with *Tc*AChE.[21]

5. Docking studies

To support the interpretation of the structure–affinity relationships and to gain more insights on the molecular determinants responsible for the observed high affinities, a careful modeling study was undertaken through molecular docking.

PDB was screened in the search of possible protein target for docking simulations. Among the available 107 AChE structures by fish, human, mouse, and other sources, docking simulations were performed on the human AChE (*h*AChE) (PDB code 1B41) rather than the more largely used *T. californica* enzyme (*Tc*AChE), because it has almost identical amino acid residues at both the catalytic and peripheral binding sites, apart from the substitution of Y337 (*human*) with P330 (*Tc*).[22] This single residue change was not observed when aligning primary sequences of both human (1B41, PDB entry) and bovine (AA123899.1, NCBI entry) AChEs.

Homo- and hetero-bivalent inhibitors **2**, **6**, **8**, **12**, **14**, and **16**, carrying a four-methylene linker, were chosen for docking studies, since they generally were more active than the corresponding lower homologous inhibitors with a three-methylene spacer. GOLD, a genetic algorithm-based software,[23] was used for docking study and the GOLDScore option was selected as the fitness function.

Docking runs basically addressed the effects on affinity of cation–π, π–π stacking, and other non-bonded interactions involving charged and aromatic molecular moieties of our inhibitors and the electron-rich W86 and W286 amino acid side chains located in the catalytic and peripheral AChE binding sites, respectively.

Moreover, we attempted to explain the dramatic loss of affinity observed by removing the two hydroxyl groups from the highly potent homobivalent inhibitor **12** yielding the low active inhibitor **16**.

Docking was first executed on the most active AChE inhibitor **12** (IC_{50} = 0.17 nM), while scaffold match constraint was adopted to perform docking simulations with the other selected inhibitors. Top-scored docking pose of **12** (50.16 kJ/mol) displayed a cation–π interaction between the trimethylammonium groups and the electron-rich side chain of W86, a highly specific hydrogen bond between the phenolic hydroxyl and an oxygen atom of the hydroxyl group of S203 (indicated by a red dashed line in Fig. 1) and a potential π–π stacking interaction between the aromatic moiety of the ligand and the aromatic ring(s) of W286 in the PAS.

Similarly, docking simulations revealed that the top-scored docking pose (58.13 kJ/mol) of the most active hetero-bivalent inhibitor **14**, displayed a binding pattern similar to that of **12** (Fig. 2). However, the π–π stacking interaction of the coumarin moiety was probably slightly weaker than the combined π–π and π–cation interactions involving the phenyl-trimethylammonium moiety. The key interactions underlying the binding of the strong inhibitors **12** and **14** took place at an optimal distance assured by a four methylene linker, in full agreement with the observed experimental affinities.

Docking results from the other analyzed inhibitors provided easily interpretable binding models (data not shown). However, the correlation of the GOLDScore values with the observed inhibitory potencies (expressed as pIC_{50}) for inhibitors **2**, **6**, **8**, **12**, **14**, and **16** was quite poor (r^2 = 0.32), confirming that docking scores are not well suited to correctly predict free binding energies.[24]

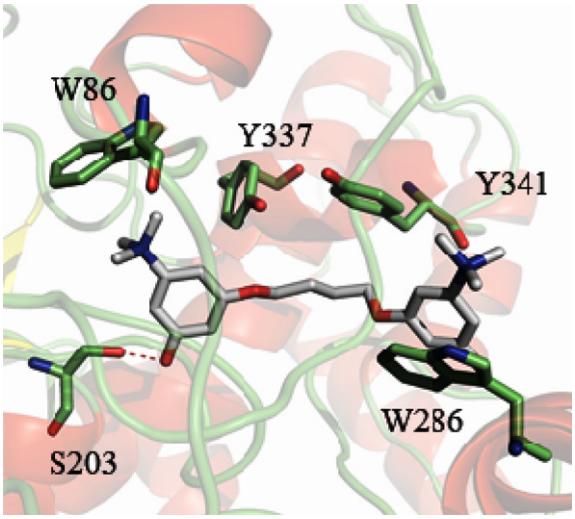

Figure 1. Top-scored docking pose of **12** into the *h*AChE binding sites.

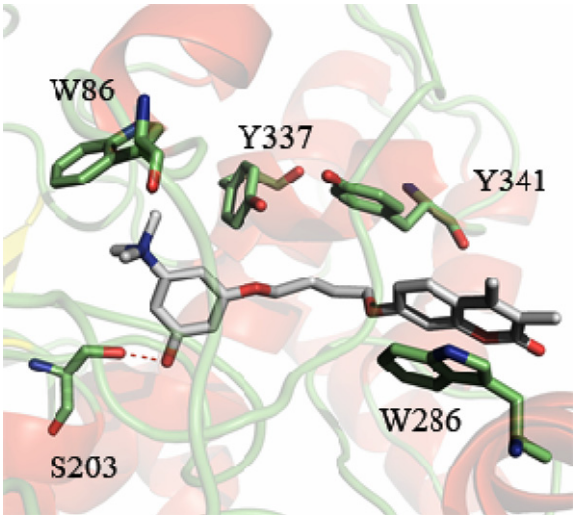

Figure 2. Top-scored docking pose of **14** into the*h*AChE binding sites.

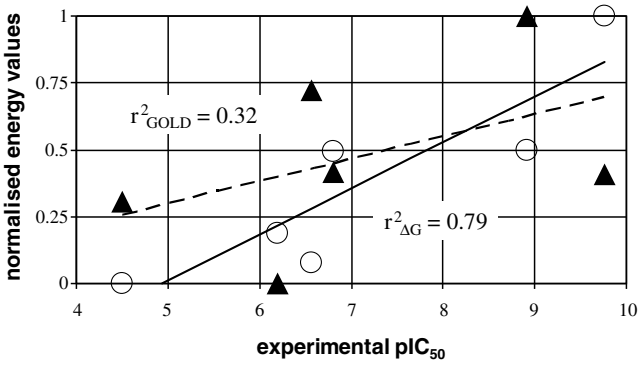

Figure 3. Linear regression of experimental pIC_{50} versus GOLDScore (filled, black triangles) and RBE (empty circles) normalized values (0–1).

Docking poses were therefore subjected to a rescoring process according to a protocol recently proposed by Jacobson.[25] Prime 1.5 module, available within Schrödinger-Maestro 7.5,[26] was used to minimize in implicit solvent (generalised Born) the protein–ligand complex ($E_{lig\text{-}prot}$) together with free ligand (E_{lig}) and protein (E_{prot}). For each ligand, the relative binding energy (RBE) was then calculated by subtracting from the energy of the ligand–protein complex the sum of the energy of the isolated protein and ligand. As expected, the linear correlation of RBE with pIC_{50} was considerably improved as can be easily seen in Figure 3 reporting both the worse ($r^2 = 0.32$) and the improved ($r^2 = 0.79$) linear regression derived by plotting experimental pIC_{50} versus normalized data (0–1) from GOLDScore (dashed line and solid triangles) and RBE (whole line and empty circles) values, respectively.

6. Conclusions

In summary, the very potent AChE inhibitors described in this work, carrying one or two quaternary ammonium groups, might have potential in the treatment of myasthenia gravis, neuromuscular blockade, and glaucoma. Taken together, our results confirm and reinforce the strategic validity of the 'fragment-based' design for the preparation of highly potent AChE inhibitors. By tethering low-affinity inhibitors with a spacer of an appropriate length, it was possible to obtain AChE inhibitors with low- to sub-nanomolar affinity. In particular, a properly substituted coumarin ring proved to be an ideal molecular entity for an optimal interaction at the PAS of AChE, as already observed by us[14] and Recanatini and co-workers.[27] This observation should be adequately considered to design dual binding site AChE inhibitors presenting a basic amino group, in the moiety binding at the catalytic site, in place of the quaternary ammonium groups examined in this work. Dual binding site AChE inhibitors of this kind might play an important role in the symptomatic treatment of AD since the interaction at PAS may inhibit the AChE induced beta-amyloid aggregation,[28] a characteristic pathological event in AD.

Lastly, modeling studies allowed an in depth analysis and interpretation of the structure–affinity relationships and increased our understanding of the main binding interactions taking place at the AChE binding sites. Besides an expected important role played by cation–π,[29] π–π stacking, hydrophobic, and other non-bonded interactions,[30] the key role of a phenolic hydroxyl forming a highly specific hydrogen bond with an oxygen atom of the hydroxyl group of Ser 203, as already observed with edrophonium,[21] was confirmed. The analysis of all these important binding interactions, well supported by a more accurate calculation of the energy of the enzyme–inhibitor complex formation, provided valuable insights for the design of new classes of potent and selective AChE inhibitors.

7. Experimental

7.1. Chemistry

Compounds **1**–**15** were prepared according to the reaction pathways illustrated in Scheme 1.[16] Amines **7**–**10** were purified before the final quaternarization reaction by flash chromatography on silica gel columns eluting with binary ethyl acetate-*n*/hexane mixtures. The purity of all the tested compounds, checked by HPLC, ^{1}H NMR, and ESI mass, was always >96%. Starting materials, reagents, and analytical grade solvents were from commercial sources. Melting point (mp) was determined only for target compound **16** by the capillary method on a Stuart Scientific SMP3 electrothermal apparatus and is uncorrected. HPLC analyses were carried with a Waters 1585 system, equipped with a model 2487 UV detector, on a Waters XTerra C8 column (3 mm × 250 mm), and different MeOH/H_2O mixtures as the mobile phase. ESI mass spectra were performed on a Agilent 1100 series LC-MSD trap system VL apparatus. Microanalyses were made only on the target final product **16** on a Euroea 3000 microanalyzer instrument; C, H, and N were within ±0.4% of the calculated values. ^{1}H NMR spectra were recorded at 300 MHz on a Varian Mercury 300 instrument. Chemical shifts are expressed in δ (ppm) and coupling constants *J* in hertz (Hz). The following abbreviations were used: s (singlet), br (broad signal), m (multiplet).

The synthesis of compound **16** was carried out according to the reaction steps depicted in Scheme 2, as follows:

7.1.1. Synthesis of 1,4-bis(3-nitrophenoxy)butane (18)

m-Nitrophenol (1.0 g, 7.2 mmol) was dissolved in 22 mL of dry CH_3CN, and then anhydrous K_2CO_3 (498 mg, 3.6 mmol) and 1,4-dibromobutane (287 μL, 2.4 mmol) were added. The mixture was refluxed for 24 h and the solvent was removed under reduced pressure. The resulting crude solid mixture was triturated with $CHCl_3$ (100 mL) and the inorganic solid residue was filtered off. The organic phase was extracted with NaOH 3 N (3 × 30 mL), dried over anhydrous Na_2SO_4, and concentrated to dryness. The resulting solid was washed with *n*-hexane and filtered, yielding 698 mg (87%) of a white-off solid with a sufficient purity for the subsequent reaction. MS (ESI) *m*/*z* 333 $(M+H)^+$; ^{1}H NMR ($CDCl_3$) δ 2.05 (br, 4H), 4.13 (br, 4H), 7.20–7.26 (m, 3H), 7.40–7.46 (m, 2H), 7.72–7.84 (m, 3H).

7.1.2. Synthesis of 3,3′-(butane-1,4-diylbis(oxy))dibenzenamine (17)

Compound **18** (332 mg, 1.0 mmol) was dissolved in 60 mL of a 1:1 mixture of ethanol/dioxane, and then Pd 'black' (60 mg) was added. The mixture was stirred for 7 h at room temperature under H_2 pressure (4 bar). The catalyst was removed by filtration through a pad of Celite®, and the solvent was removed under vacuum yielded the desired product as a yellow oil with acceptably high purity (248 mg, 91% yield). MS (ESI) *m*/*z* 318 $(M+2Na)^+$; ^1H NMR ($CDCl_3$) δ 1.93 (br, 4H), 3.98 (br, 4H), 3.50 (br, 4H), 6.24–6.33 (m, 6H), 7.02–7.07 (m, 2H).

7.1.3. Synthesis of 3,3′-(butane-1,4-diylbis(oxy))bis(*N,N,N*-trimethylbenzenaminium iodide) (16)

Diamine **17** (100 mg, 0.37 mmol) was dissolved in ethanol (3.0 mL), and then anhydrous K_2CO_3 (102 mg, 0.74 mmol) and methyl iodide (230 μL, 3.7 mmol) were added. The mixture was refluxed for 2 h, filtered, and the filtrate was concentrated to dryness. The resulting crude solid was crystallized from dry ethanol yielding 84 mg (37%) of the title ammonium salt. Mp 172–175 °C dec. Found: C, 43.50; H, 5.60; N, 4.63. $C_{22}H_{34}I_2N_2O_2$ requires C, 43.15; H, 5.60; N, 4.57%; ^1H NMR (DMSO-d_6) δ 1.90 (br, 4H), 3.56 (s, 18H), 4.13 (br, 4H), 7.15–7.17 (m, 2H), 7.45–7.56 (m, 6H).

7.2. Cholinesterase inhibition assay

The inhibition assays on AChE, from bovine erythrocytes (0.36 U/mg), and BChE from equine serum (13 U/mg) were run in phosphate buffer 0.1 M, at pH 8.0. Acetyl- and butyryl-thiocoline iodides were used as substrates and 5,5′-dithiobis(2-nitrobenzoic acid) (DTNB) as the chromophoric reagent. Inhibition assays were carried out on an Agilent 8453E UV–visible spectrophotometer equipped with a cell changer. AChE inhibitory activity was determined in a reaction mixture containing 200 μL of a solution of AChE (0.415 U/mL in 0.1 M phosphate buffer, pH 8.0), 100 μL of a 3.3 mM solution of DTNB in 0.1 M phosphate buffer (pH 7.0) containing 6 mM $NaHCO_3$, 100 μL of a solution of the inhibitor (five to seven concentrations ranging from 1×10^{-11} to 1×10^{-4} M), and 500 μL of phosphate buffer, pH 8.0. After incubation for 20 min at 25 °C, acetylthiocholine iodide (100 μL of 0.05 mM water solution) was added as the substrate, and AChE-catalyzed hydrolysis was followed by measuring the increase of absorbance at 412 nm for 3.0 min at 25 °C. The concentration of compound which determined 50% inhibition of the AChE activity (IC_{50}) was calculated by non-linear regression of the response–concentration (log) curve, using GraphPad Prism v. 4.0. BChE inhibitory activity was assessed similarly using butyrylthiocholine iodide (0.05 mM) as the substrate.

7.3. Computational studies

Computational analyses were conducted on a 16 nodes Linux Cluster employing an openMosix® architecture composed by AMD Athlon XP 2400^+ and Intel Xeon 2600 cpu_s. All the molecules were built from the Sybyl fragment libraries.[31] Geometrical optimization and charge calculation were carried out by means of a quantum mechanical method with the PM3 Hamiltonian. Molecules and models were displayed and manipulated on a Silicon Graphics O^{2+} machine. The docking poses reported in Figures 1 and 2 were prepared with the graphic system PyMol.[32]

7.4. Docking simulations

The target protein was prepared by adding hydrogen atoms, completing and optimizing missing residues, removing water and the cocrystallized fasciculin molecule from the *h*AChE crystallographic complex coded 1B41 in the PDB. Using the *Protein Preparation* module of Maestro software,[26] a light relaxation was performed for optimizing first hydroxyl and thiol torsion angles followed by an all-atom constrained minimization to remove steric clashes until the RMSD reached a value of 0.18 Å.

GOLD 2.2, a genetic algorithm-based software, was used in the docking study selecting the GOLDScore as the fitness function. GOLDScore is made up of four components that account for protein–ligand binding energy: protein–ligand hydrogen bond energy (*external H-bond*), protein–ligand van der Waals energy (*external vdw*), ligand internal vdw energy (*internal vdw*), and ligand torsional strain energy (*internal torsion*). Empirical parameters used in the fitness function (hydrogen bond energies, atom radii and polarizabilities, torsion potentials, hydrogen bond directionalities, and so forth) were taken from the GOLD parameter file. The fitness score is taken as the negative of the sum of the energy terms, so that larger fitness scores indicated a better binding. The fitness function has been optimized for the prediction of ligand binding positions rather than the prediction of binding affinities, although some correlation with the latter can also be found. The protein input file may be the entire protein structure or a part of it comprising only the residues which are in the region of the ligand binding site. In this study, GOLD was allowed to calculate interaction energies within a sphere of a 14 Å centered on the middle of the four-methylene spacer.

Acknowledgment

The authors gratefully thank MUR, Rome, Italy (PRIN, 2006) for financial support.

References and notes

1. Lane, R. M.; Potkin, S. G.; Enz, A. *Int. J. Neuropsychopharmacol.* **2006**, *9*, 101.
2. Zimmerman, G.; Soreq, H. *Cell Tissue Res.* **2006**, *326*, 655.
3. Abraham, D. J., 6th ed.. In *Anticholinergic Drugs in Burger's Medicinal Chemistry and Drug Discovery*; Wiley: New York, 2003; Vol. 6,. ch 4.
4. Giacobini, E. *Pharmacol. Res.* **2004**, *50*, 433.
5. Sussman, J. L.; Harel, M.; Frolow, F.; Oefner, C.; Goldman, A.; Toker, I.; Silman, I. *Science* **1991**, *253*, 872.
6. Berman, H. M.; Westbrook, J.; Feng, Z.; Gilliland, G.; Bhat, T. N.; Weissig, H.; Shindyalov, I. N.; Bourne, P. E. *Nucleic Acids Res.* **2000**, *28*, 235.
7. Du, D. M.; Carlier, P. R. *Curr. Pharm. Des.* **2004**, *10*, 3141.
8. Li, W. M.; Kan, K. K.; Carlier, P. R.; Pang, Y. P.; Han, Y. F. *Cur. Alzheimer Res.* **2007**, *4*, 386.
9. Camps, P.; Munoz-Torrero, D. *Mini-Rev. Med. Chem.* **2001**, *1*, 163.
10. (a) Pang, Y. P.; Quiram, P.; Jelacic, T.; Hong, F.; Brimijoin, S. *J. Biol. Chem.* **1996**, *271*, 23646; (b) Carlier, P. R.; Han, Y. F.; Chow, E. S. H.; Li, C. P. L.; Wang, H.; Lieu, T. X.; Wong, H. S.; Pang, Y. P. *Bioorg. Med. Chem.* **1999**, *7*, 351; (c) Hu, M. K.; Wu, L. J.; Hsiao, G.; Yen, M. H. *J. Med. Chem.* **2002**, *45*, 2277; (d) Rydberg, E. H.; Brumshtein, B.; Greenblatt, H. M.; Wong, D. M.; Shaya, D.; Williams, L. D.; Carlier, P. R.; Pang, Y. P.; Silman, I.; Sussman, J. L. *J. Med. Chem.* **2006**, *49*, 5491; (e) Campiani, G.; Fattorusso, C.; Butini, S.; Gaeta, A.; Agnusdei, M.; Gemma, S.; Persico, M.; Catalanotti, B.; Savini, L.; Nacci, V.; Novellino, E.; Holloway, H. W.; Greig, N. H.; Belinskaya, T.; Fedorko, J. M.; Saxena, A. *J. Med. Chem.* **2005**, *48*, 1919; (f) Carlier, P. R.; Du, D. M.; Han, Y. F.; Liu, J.; Perola, E.; William, I. D.; Pang, Y. P. *Angew. Chem., Int. Ed.* **2000**, *39*, 1775.
11. (a) Carlier, P. R.; Chow, E. S.; Han, Y.; Liu, J.; Ek Yazal, J.; Pang, Y. P. *J. Med. Chem.* **1999**, *42*, 4225; (b) Gemma, S.; Gabellieri, E.; Huleatt, P.; Fattorusso, C.; Borriello, M.; Catalanotti, B.; Butini, S.; De Angelis, M.; Novellino, E.; Nacci, V.; Belinskaya, T.; Saxena, A.; Campiani, G. *J. Med. Chem.* **2006**, *49*, 3421; (c) Elisinghorst, P. W.; Tanarro, C. M.; Gutschow, M. *J. Med. Chem.* **2006**, *49*, 7540.
12. Kryger, G.; Silman, I.; Sussman, J. L. *Struct. Fold Des.* **1999**, *7*, 297.
13. Seltzer, B. *Expert Opin. Pharmacother.* **2007**, *8*, 1011.
14. Brühlmann, C.; Ooms, F.; Carrupt, P. A.; Testa, B.; Catto, M.; Leonetti, F.; Altomare, C.; Carotti, A. *J. Med. Chem.* **2001**, *44*, 3195.
15. Hajduk, P. J.; Greer, J. *Nat. Rev. Drug Disc.* **2007**, *6*, 211.
16. Leonetti, F.; Cappa, A.; Maccallini, C.; Carotti, A. *Arkivoc* **2004**, *5*, 272.
17. Ellman, G. L.; Courtney, K. D.; Andres, V., Jr.; Featherstone, R. M. A. *Biochem. Pharmacol.* **1961**, *7*, 88.
18. Hodge, A. S.; Humphrey, D. R.; Rosenberry, T. L. *Mol. Pharmacol.* **1992**, *41*, 931.
19. Atack, J. R.; Yu, Q. S.; Soncrant, T. T.; Brossi, V.; Rapoport, S. I. *J. Pharmacol. Exp. Ther.* **1989**, *249*, 194.
20. Camps, P.; Gómez, E.; Muñoz-Torrero, D.; Badia, V.; Clos, M. V.; Curutchet, C.; Muñoz-Muriedas, V.; Luque, F. G. *J. Med. Chem.* **2006**, *49*, 6833.

21. Ravelli, R. B.; Raves, M. L.; Ren, Z.; Bourgeois, D.; Roth, M.; Kroon, J.; Silman, I.; Sussman, J. L. *Acta Crystallogr.* **1998**, *4*, 1359.
22. Barril, X.; Orzoco, M.; Luque, F. J. *J. Med. Chem.* **1999**, *42*, 5110.
23. Verdonk, M. L.; Cole, J. C.; Hartshorn, M. J.; Murray, C. W.; Taylor, R. D. *Proteins* **2003**, *52*, 609.
24. Warren, G. L.; Andrews, C. W.; Capelli, A. M.; Clarke, B.; La Londe, J.; Lambert, M. H.; Lindvall, M.; Nevins, N.; Semus, S. F.; Senger, S.; Tedesco, G.; Wall, I. D. *J. Med. Chem.* **2006**, *49*, 5912.
25. Kalyanaraman, C.; Bernacki, K.; Jacobson, M. P. *Biochemistry* **2005**, *44*, 2059.
26. Maestro7.5, Schrödinger Inc., Portland, OR 97201, USA.
27. Piazzi, L.; Rampa, A.; Bisi, A.; Gobbi, S.; Belluti, F.; Cavalli, A.; Bartolini, M.; Andrisano, V.; Valenti, P.; Recanatini, M. *J. Med. Chem.* **2003**, *46*, 2279.
28. Bartolini, M.; Bertucci, C.; Cavrini, V.; Andrisano, V. *Biochem. Pharmacol.* **2003**, *65*, 407.
29. Zacharias, N.; Dougherty, D. A. *Trends Pharmacol. Sci* **2002**, *23*, 281.
30. Imai, Y. N.; Inoue, Y.; Yamamoto, Y. *J. Med. Chem.* **2007**, *50*, 1189.
31. SYBYL7.2 Tripos Inc., St. Louis, MO 63144.
32. The PyMOL Molecular Graphics System; DeLano Scientific: San Carlos, CA, USA.